APPLICATION OF A NOVEL PID AUTO-TUNER TO A LUNG FUNCTION TESTING DEVICE

Andres Hernandez, Robin De Keyser and Clara Ionescu
Department of Electrical energy, Systems and Automation, Ghent University
Technologiepark 913, B9052 Gent, Ghent, Belgium
{ClaraMihaela.Ionescu, Robain.DeKeyser}@UGent.be

Keywords: Respiratory impedance, Closed loop control, PID, Auto-tuner, Frequency response.

Abstract: The paper presents a closed loop approach for the lung function tests of forced oscillation technique. In this method it is important to ensure that the desired excitation signal to be applied at the patient's mouth will be delivered by the lung function testing device, without introducing distortions and nonlinear effects. A novel PID auto-tuner is applied in an initial phase of the investigation, without the patient, to verify whether the closed loop control can be implemented. The results are promising, showing that the auto-tuner is able to perform well and ensure the desired signal at the output of the device, within safety limits for the control effort (air flow).

1 INTRODUCTION

Non-invasive lung function tests are broadly used for assessing respiratory mechanics (Northrop, 2002; Oostveen *et al.,* 2003). Contrary to the forced maneuvers from patient side and special training for the technical medical staff necessary in spirometry and in body plethysmography (Pellegrinno *et al.,* 2005; Miller *et al.,* 2005), the technique of superimposing air pressure oscillations is simple and requires minimal cooperation from the patient, during tidal breathing (Oostveen *et al.*, 2003). Among the air pressure oscillation techniques for lung function testing, the most popular one is that of Forced Oscillation Technique (FOT). FOT uses a multisine signal to excite the respiratory mechanical properties over a wide range of frequencies, usually between 4-48Hz (Oostveen *et al.,* 2003).

Using measurements of air pressure and air flow, it is possible to extract information regarding the human respiratory input impedance. However this is a linear approximation of a nonlinear system, hence the output will depend on the input's amplitude and frequency (Schoukens & Pintelon, 2001). It is therefore important to ensure that the desired signal to be applied at the patient's mouth will be delivered by the lung function testing device, without introducing distortions and nonlinear effects. Hence, a closed loop control system is necessary, to continuously monitor and correct the errors between the desired input signal and the one delivered by the device at the patient's mouth.

PID controllers can incorporate *auto-tuning* capabilities (Åström & Hägglund, 1995). The auto-tuners are equipped with a mechanism capable of automatically computing a reasonable set of parameters when the regulator is connected to the process. Auto-tuning is a very desirable feature because it does not require a-priori identification of the system to be controlled. The auto-tuning features provide easy-to-use controller tuning and have proven to be well accepted among process engineers (Leva *et al*. 2002).

The aim of this study is to apply a PID auto-tuner to the FOT device and test whether the controller can follow a multisine reference input. The objective is that the nonlinear effects and distortions coming from the FOT device itself are corrected by the control action, such that the excitation signal of interest is delivered to the patient. In this incipient phase, the closed loop control will be designed for a hypothetical patient: a respiratory tube and a rubber balloon. The underlying reason is that we need to ensure repeatability of our experiments, in order to check the feasibility of implementing a closed loop control strategy in the lung function device. The final aim is to develop the closed loop control for the case when the patient is breathing (i.e. in presence of disturbance).

The paper is organized as follows: the device and test setup are described in the next section. The underlying principles of the auto-tuner algorithm and the PID parameters are given in the third section, followed by a section describing the validation of the closed loop control for multisine setpoint and comparison to open loop performance. A conclusion section summarizes the main outcome of this investigation and points towards further developments.

2 IMPEDANCE MEASUREMENT

The impedance was measured using a modified FOT setup, able to assess the respiratory mechanics from 4-50 Hz. The specifications of the device are: 11kg, 50x50x60 cm, 40 seconds measurement time, European Directive 93/42 on Medical devices and safety standards EN60601-1.

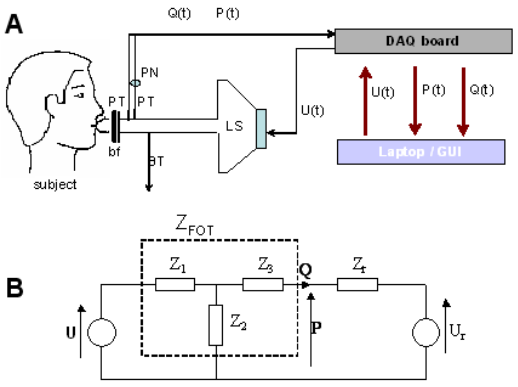

Figure 1: A schematic overview (**A**) and an electrical analogy of the FOT setup (**B**).

Typically for lung function testing purposes, the subject is connected to the setup from figure 1 via a mouthpiece, suitably designed to avoid flow leakage at the mouth and dental resistance artefact. The oscillation pressure is generated by a loudspeaker (LS) connected to a chamber. The LS is driven by a power amplifier fed with the oscillating signal generated by a computer. The movement of the LS cone generates a pressure oscillation inside the chamber, which is applied to the patient's respiratory system by means of a tube connecting the LS chamber and the bacterial filter (bf). A side opening of the main tubing (BT) allows the patient to have fresh air circulation. Ideally, this pipeline will have high impedance at the excitation frequencies to avoid the loss of power from the LS pressure chamber. It is advisable that during the measurements, the patient wears a nose clip and keeps the cheeks firmly supported. Before starting the measurements, the frequency response of the pressure transducers (PT) and of the pneumotachograph (PN) are calibrated. The PN is a meter for measuring gas flow rates during breathing by recording pressure differences across a device of fixed-flow resistance that has known pressure and flow characteristics. The measurements of air-pressure **P** and air-flow **Q** during the FOT lung function test are done at the mouth of the patient.

The FOT excitation signal was kept within a range of a peak-to-peak range of 0.1-0.3 kPa, in order to ensure patient comfort and linearity (Oostveen *et al.*, 2003). From these signals, the non-parametric representation of the patient's lung impedance Z_r is obtained assuming a linear dependence between the breathing and superimposed oscillations at the mouth of the patient (Ionescu & De Keyser, 2008). The algorithm for estimating Z_r can be summarized from the electrical analogue in figure 1-B:

$$P(s) = Z_r(s)Q(s) + U_r(s) \tag{1}$$

where s denotes the Laplace operator. Since the excitation signal is designed such that it is not correlated with the breathing of the patient, correlation analysis can be applied to the measured signals. Therefore, one can estimate the respiratory impedance as the ratio:

$$Z_r(j\omega) = \frac{S_{PU}(j\omega)}{S_{QU}(j\omega)} \tag{2}$$

whereas the **P** corresponds to pressure (its electrical equivalent is voltage) and **Q** corresponds to air-flow (its electrical equivalent is current), **U** the excitation signal, $S_{ij}(j\omega)$ the cross-correlation spectra between the various input-output signals, ω is the angular frequency and $j = (-1)^{1/2}$, resulting in the complex variable Z_r. From the point of view of the forced oscillatory experiment, the signal components of respiratory origin (U_r) have to be regarded as pure noise for the identification task (Ljung, 1999). In this application, the patient is replaced by a system without disturbance U_r=0 (i.e. a respiratory tube with a rubber balloon attached at the end) in order to ensure repeatability and test the feasibility of implementing a closed loop control algorithm in the FOT setup.

3 UNDERLYING PRINCIPLES OF KCR PID AUTO-TUNING

The development of this auto-tuning algorithm is based on the prior art where two relay-based PID auto-tuners have been presented: the Kaiser-Chiara auto-tuner and the Kaiser-Rajka auto-tuner. Hence the proposed algorithm is an extended combination of the two: the Kaiser-Chiara-Rajka auto-tuner algorithm (KCR) (De Keyser & Ionescu, 2010). Notice that the development of the PID controller does not require a-priori knowledge of the system.

The closed loop transfer function of a second order system with complex conjugate poles, and static gain one is given by:

$$T(s) = \frac{\omega_n^2}{s^2 + 2\zeta\omega_n s + \omega_n^2} \tag{3}$$

with ω_n the natural frequency and ζ the damping factor. From (3) one has the relationship between the closed loop percent overshoot (*OS%*) and the peak magnitude M_p in frequency domain (Nise, 2007):

$$\%OS = 100e^{-\pi/\sqrt{1-\zeta^2}},\ M_p = \frac{1}{2\zeta\sqrt{1-\zeta^2}} \tag{4}$$

By specifying the allowed overshoot in the closed loop, it follows that the closed loop transfer function must fulfill the condition:

$$\left|T(j\omega)\right| = \left|\frac{G(j\omega)}{1+G(j\omega)}\right| = M_p \tag{5}$$

with $G(j\omega)$ the open loop transfer function of both the process and controller. Re-writing (5) in its complex form:

$$T(j\omega) = \frac{R(\omega) + jI(\omega)}{\left[1+R(\omega)\right] + jI(\omega)} \tag{6}$$

with *R* the real part and *I* the imaginary part, and taking $\left|T(j\omega)\right|^2$ results that:

$$\left(R+c\right)^2 + I^2 = r^2 \tag{7}$$

where $c = \frac{M_p^2}{M_p^2-1}$, $r = \frac{M_p}{M_p^2-1}$, which is nothing else than the equation of a (Hall-)circle with radius *r* and center in $\{-c, 0\}$ (Nise, 2007). In order to have a peak magnitude, only those circles with *M*>1 are of interest. Intersection with the unit circle is achieved by using (7) and the condition: $R^2 + I^2 = 1$, hence solving for *R* and *I* yields:

$$R = 0.5\frac{1-2M_p^2}{M_p^2} \text{ and } I = -\frac{\sqrt{M_p^2 - 0.25}}{M_p^2} \tag{8}$$

The phase margin is given by $\tan PM = \frac{|I|}{|R|}$ thus:

$$PM = \tan^{-1}\frac{\sqrt{M_p^2 - 0.25}}{M_p^2 - 0.5} \tag{9}$$

We stated in (De Keyser & Ionescu, 2010) that specifying *PM* does not suffice to guarantee a good closed loop performance in all situations. Therefore, the next step is to determine the cross-over frequency; i.e. the frequency where the process and controller crosses the 0 dB line (open loop).

If the settling time of the closed loop is specified, then using $T_s = 4/\omega_n\zeta$ and (4) we can obtain the bandwidth frequency:

$$\omega_{BW} = \omega_n\sqrt{\left(1-\zeta^2\right) + \sqrt{4\zeta^4 - 4\zeta^2 + 2}} \tag{10}$$

From (De Keyser & Ionescu, 2010), we use that $\omega_{BW} \approx 1.5\omega_c$ and the generalization to higher order systems which gives $\omega_c \le \omega_{BW} \le 2\omega_c$. By having the cross-over frequency ω_c, a sinusoid with period $T_c = \frac{\omega_c}{2\pi}$ can be applied to the process and obtain the output:

$$G(j\omega_c) = Me^{j\varphi} = M\left(\cos\varphi + j\sin\varphi\right) \tag{11}$$

using the transfer function analyzer algorithm (Ionescu *et al*, 2010). The task is now to find the controller parameters such that the specification for phase margin is fulfilled, by giving $\%OS$, T_s, M and φ.

The controller is derived in its *textbook* form, which for the critical frequency becomes:

$$R(j\omega_c) = K_p\left[1 + j\left(T_d\frac{2\pi}{T_c} - \frac{1}{T_i\frac{2\pi}{T_c}}\right)\right] \tag{12}$$

Starting from the controller frequency response in (12), the loop frequency response is given by:

$$R(j\omega_c)G(j\omega_c) = 1 \cdot e^{j(-180°+PM)} \\ = \cos(-180° + PM) + j \cdot \sin(-180° + PM) \\ = -a - jb \quad (13)$$

with $a = \cos PM$ and $b = \sin PM$, schematically shown in figure 2.

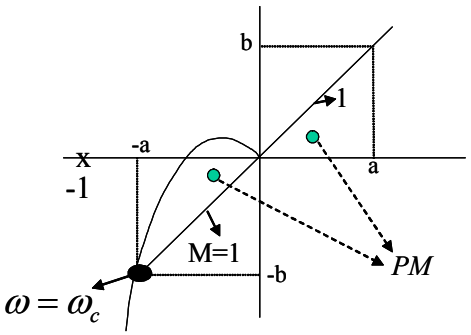

Figure 2: Schematic of the KCR tuning principle.

Based on (12), the controller is given by:

$$R(j\omega_c) = \left[1 + j\left(T_d\omega_c - \frac{1}{T_i\omega_c}\right)\right] = K_p(1 + j\alpha) \quad (14)$$

Equivalence of (13) with (14) gives that

$$K_p M\left[(\cos\varphi - \alpha\sin\varphi) + j(\sin\varphi + \alpha\cos\varphi)\right] \\ = -(\cos PM + j\sin PM) \quad (15)$$

From the real and imaginary parts of (15), we have that:

$$\alpha = \frac{\tan PM - \tan\varphi}{1 + \tan PM\tan\varphi} = \tan(PM - \varphi) \\ = T_d\omega_c - \frac{1}{T_i\omega_c} \quad (16)$$

and using T_i=4T_d, (16) becomes:

$$T_d\omega_c - \frac{1}{4T_d\omega_c} = \tan(PM - \varphi) \quad (17)$$

from where

$$T_i = T_c\frac{\sin(PM - \varphi) \pm 1}{\pi\cos(PM - \varphi)} \quad (18)$$

which gives only one positive result. From (15) and (16) we have that

$$\left(K_p M\right)^2 * (1 + \alpha) = 1, \quad (19)$$

With

$$1 + \alpha^2 = 1 + \tan^2(PM - \varphi) = \frac{1}{\cos^2(PM - \varphi)} \quad (20)$$

which gives the K_p controller parameter:

$$K_p = \pm\frac{\cos(PM - \varphi)}{M} \quad (21)$$

with only one positive result.

4 CONTROLLER VALIDATION

4.1 Open Loop Identification

In order to verify the performance of the controller, we shall identify the open loop frequency response of the system. We shall make use of the Chirp-TFA (Chirp Transfer Function Analyzer) technique proposed in (Ionescu *et al.,* 2010). In short, the frequency of such a sinusoidal test signal varies from a minimum frequency (f_0) until a maximum frequency (f_1) in a certain time (t_1), known as a chirp signal. In the Chirp-TFA framework, the sampling period varies such that a fixed number of samples per period are ensured (N_s), independent of the increasing frequency.

An example of a chirp signal with fixed number of samples per period is given in figure 3. Notice that the sampling period will be adjusted at every sampling instant, because the frequency is varying continuously. After the measurement is performed, in order to process the data, the chirp signal is divided into sections, such that sub-sequent sections which have approximately the same frequency. Each of these sections will be used to obtain one point for gain and one point for the phase in the Bode diagram of the system. The schematic flowchart of the Chirp-TFA discrete-time implementation is depicted in figure 4.

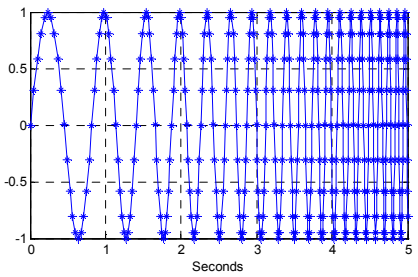

Figure 3: Chirp signal from 1 to 10 Hz in 5 seconds, 20 samples per period.

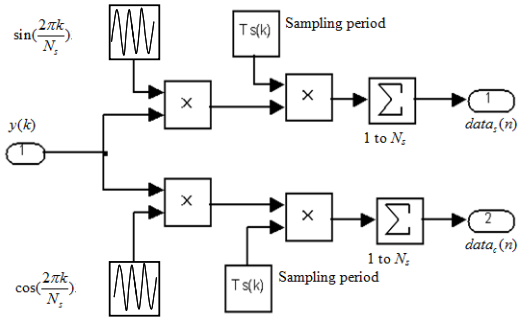

Figure 4: Scheme of the Chirp-TFA discrete implementation.

The form of the chirp signal is given by $\sin(2\pi \cdot f \cdot t) = \sin(2\pi \cdot f(t) \cdot kT_s(t))$. Hence, at every time instant *t*, a variable sampling period $T_s(t)$ is calculated, such that one period contains N_s samples. The relation is given by $f(t) \cdot T_s(t) = \frac{1}{N_s}$.

The N_s samples are then given by $\sin(\frac{2\pi k}{N_s})$, with k=0, 1… N_s -1. The sinusoidal output of a system in terms of its magnitude, phase and noise, can be written as:

$$y(k) = b\sin(2\pi k / N_s + \varphi) + n(k) \tag{22}$$

where n is the noise, b is the amplitude, ω is the angular frequency and φ is the phase shift. For example, at the n^{th} interval, we have that:

$$data_s(n) = \sum_{k=N_s(n-1)}^{N_s n-1} y(k)\sin(\frac{2\pi k}{N_s})T_s(k) \tag{23}$$

$$data_c(n) = \sum_{k=N_s(n-1)}^{N_s n-1} y(k)\cos(\frac{2\pi k}{N_s})T_s(k) \tag{24}$$

where $T_s(k)$ represents the sampling period at the k^{th} sample in the data vector and:

$$T_s(k) = \frac{1}{N_s f(k)} \tag{25}$$

where $f(k)$ denotes the frequency at the k^{th} sample. Considering that we obtain one point in a Bode plot for each period on which we integrate, it makes sense to increase the frequency exponentially with time, in order to get the same resolution (points per decade) for all frequency intervals in the plot. Therefore, the frequency points are calculated from:

$$f(t) = f_0(\frac{f_1}{f_0})^{\frac{t}{t_1}} \tag{26}$$

which is then a function of the design parameters. As the measurement time T_m increases, (24) and (25) can be reduced to the approximations:

$$data_s(T_m) \approx \frac{b}{2}T_m\cos\varphi\,,\ data_c(T_m) \approx \frac{b}{2}T_m\sin\varphi \tag{27}$$

from where it follows that

$$b = \frac{2}{T_m}\sqrt{data_s^{\,2}(T_m) + data_c^{\,2}(T_m)} \tag{28}$$

$$\varphi = \arctan\frac{data_c(T_m)}{data_s(T_m)} \tag{29}$$

Plotting the *b/a* and φ values for a range of frequencies provides the Bode diagram for the observed system.

4.2 Real-time Implementation

In practice, in order to send a sinusoidal signal of 50 Hz, is necessary to have a sample rate for about 500 Hz, which means about 10 samples per sinusoid period. The sampling time obtained was 0.002 seconds. In this particular example, it is not possible to work with Matlab, because the delay for calculations in the closed loop is about 14ms, much higher than the desired sample rate. A solution to overcome this limitation consists in using Real Time Windows Target (RTWT) Toolbox in Matlab. This toolbox assigns some resources of the system exclusively for this task, ensuring the desired sampling time. A corresponding Simulink model was developed in order to send and receive signals to/from the real FOT system, as depicted in figure 5. Next, the Simulink model is automatically compiled in C-language, making in this way a direct communication using the National Instruments DAQCard 6024E (which is recognized by Matlab and supported for real time applications).

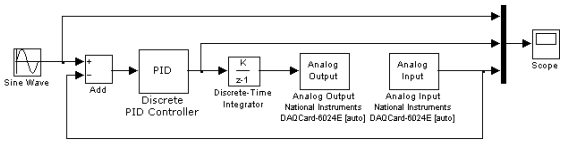

Figure 5: Real Time Simulink model used in closed loop.

4.3 Open Loop versus Closed Loop Performance

The open loop and closed loop identification using the Chirp-TFA algorithm is given by means of Bode plots in figure 6. It can be observed that the bandwidth (frequency at -3dB) of the system is about 45Hz.

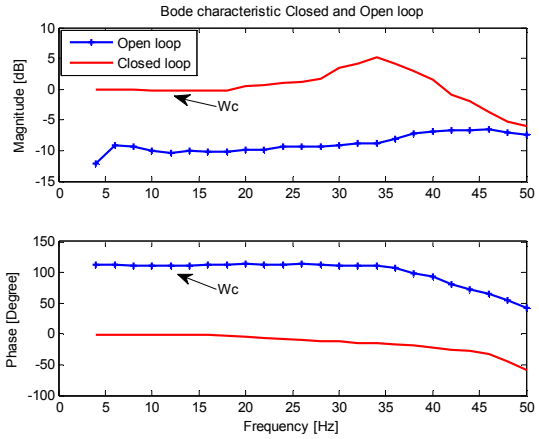

Figure 6: Bode characteristic of the open and closed loop.

For this preliminary study an OS%=20 and Ts=0.041 seconds are defined as design specifications. The KCR experiment is based on obtaining the magnitude and phase of the system for ω_c (crossover frequency), or represented in time as T_c. This value is obtained from the settling time as $T_s<T_c<2*T_s$, it follows that T_c=0.082 seconds, with ω_c=*76.62 rad/s* or *12.19 Hz*. A sinusoidal signal to this frequency ω_c was applied to the system, from where the magnitude (M) and phase (φ) were 10.48 dB, and 11.21° respectively.

Once the values for OS%, T_s are defined and M and φ are experimentally obtained, then by using (4,9, 18, 21) as presented on the KCR algorithm in section 3, it follows that the PID parameters are:

$$K_p=0.4775;\ T_i=0.0141;\ T_d=0.0035 \qquad (30)$$

The designed PID controller (30), was tested by applying a multisine setpoint with frequencies of 3Hz and 20Hz. The response is presented in figure 7.

In order to be able to follow a reference signal in a closed loop is necessary that the magnitude of the closed loop remains in 0dB and the phase in 0º into the frequencies of interest. From the Bode plot in figure 6 for the closed loop, we can observe that the results are in agreement with the expected bandwidth, and that the controller performs satisfactorily. This result is also visible when a comparison in time domain between open loop and

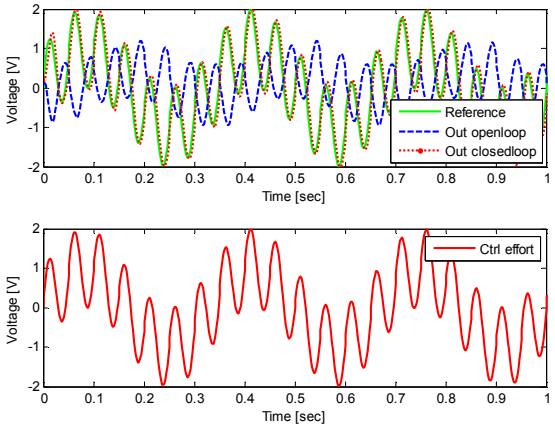

Figure 7: Comparison test between Open loop and PID controller performance for a multisine setpoint at 3 Hz and 20 Hz.

closed loop is done. The controller avoids distortions and nonlinear effects at the output of the lung function device; the desired signal will be successfully delivered at the patient's mouth as depicted in figure 7.

5 CONCLUSIONS

In this paper, the problem of closed loop control of a medical device for lung function testing was initiated. Preliminary results show that a proposed PID autotuner can be applied and developed with desired closed loop performance specifications for settling time and overshoot. The next step is to develop the method in the presence of noise, i.e. interference with the breathing signal coming from the patient.

REFERENCES

Åström, K. J., & Hägglund, T., 1995. *PID Controllers: Theory, Design and Tuning*. Instrument Society of America, Research Triangle Park, NC, USA,

De Keyser R., Ionescu C., 2010. "A generally valid algorithm for PID auto-tuners", accepted for presentation at the *Int Conf of Mathematical Methods in Engineering*, Coimbra, Portugal, to be held 21-24 October.

De Keyser R., Ionescu C., 2006. "FRtool: a frequency response tool for CACSD in MatLab", *IEEE Conf on Computer Aided Control Systems Design (CACSD-CCA-ISIC),* Munchen, Germany, pp. 2276-2280

Ionescu, C. & De Keyser, R., 2008. Parametric models for characterizing the respiratory input impedance. *Journal of Medical Engineering & Technology*, Taylor & Francis, 32(4), pp. 315-324

Ionescu C., Robayo F., De Keyser R., Naumovic M., 2010. "The frequency response analysis revisited", in *Proc. the IEEE 18th Mediterranean Conference on Control and Automation*, 23-25 June, Marrakesh, Marocco, pp. 1441-1446

Leva, A., Cox C. & Ruano A., 2002. "Hands-on Pid autotuning: a guide to better utilisation". *IFAC Professional Brief*

Ljung, L., 1999, *System Identification,* NJ: Prentice Hall

Northrop R., 2002. *Non-invasive measurements and devices for diagnosis*, CRC Press

Miller, M., Hankinson, J., Brusasco, V., Burgos, F., Casaburi, R., Coates, A., Crapo, R., Enright, P., van der Grinten, C., Gustafsson, P., Jensen, R., Johnson, D., MacIntyre, N., McKay, R., Navajas, D., Pedersen, O., Pellegrino, R., Viegi, G., Wanger, J., 2005, Standardization of spirometry, *Eur Resp J*, 26, 319-338

Nise, N. S, 2007. *Control systems engineering,* Wiley India Pvt. Ltd., 4th edition

Oostveen, E., Macleod, D., Lorino, H., Farré, R., Hantos, Z., Desager, K., Marchal, F, 2003, The forced oscillation technique in clinical practice: methodology, recommendations and future developments, *Eur Respir J*, 22, 1026-1041

Pellegrino, R., Viegi, G., Brusasco, V., Crapo, R., Burgos, F., Casaburi, R., Coates, A., van der Grinten, C. P. M., Gustafsson, P., Hankinson, J., Jensen, R., Johnson, D. C., McKay, R., Miller, M. R., Navajas, D., Pedersen, O. F., Wanger, J., 2005, Interpretative Strategies for Lung Function Tests. *European Respiratory Journal*, 26: 948-968

Schoukens J., and Pintelon, R., *System Identification, a frequency-domain approach*, (IEEE Press, 2001)